Surface Science 204 (1988) 568–586
North-Holland, Amsterdam

IMAGING GAS CONCENTRATION IN THE FIELD ION MICROSCOPE: A THEORETICAL ANALYSIS

Caio M.C. DE CASTILHO

Cavendish Laboratory, Cambridge, CB3 0HE, UK
and
Instituto de Fisica, UFBa, Campus da Federação, 40 210 Salvador, Bahia, Brazil

and

David R. KINGHAM

VG Ionex Ltd., Maltings Park, Burgess Hill, West Sussex, RH15 9TQ, UK

Received 9 February 1988; accepted for publication 2 June 1988

A Boltzmann equation method for calculating the gas concentration in the field ion microscope is proposed. A simple model for the molecule's bouncing movement is presented. Numerical results are given and the formation of an imaging gas adsorbed layer is discussed. Within this model, no evidence is found which suggests that local variation in imaging gas concentration is the basic mechanism of image formation in the FIM. The results show limits on the values of tip field and or tip temperature, for which an adsorbed layer can be formed.

1. Introduction

Theoretical explanations of image formation, resolution and contrast in the field ion microscope (FIM) have been presented in two ways which differ in the basic mechanism for the local variation in the ion production rate: (i) electron transition rate constant and (ii) imaging gas concentration [1–6]. Using a dynamical theory, van Eekelen [7] considered the gas distribution in the region close to the FIM tip deriving such quantities as the gas supply function and the total ion current and discussing the accommodation process. Iwasaki and Nakamura [8,9], using a dynamic as well as a quasi-static approach, have calculated quantities such as the number of particles arriving at the metal tip as a function of velocity, and the total ion current and capture probability as a function of tip and gas temperature, electric field and gas atom to metal atom mass ratio. Our aim is to develop a simple theoretical model for the gas concentration, considering the collision process between the imaging gas molecule (usually a single atom) and the tip surface and taking

0039-6028/88/$03.50

into account the possibility of field ionization when the imaging gas molecule passes through the ionization zone. The model is one-dimensional and the collision process will be treated classically. Despite the simplicity of the model, the formation of an adsorbed layer of the imaging gas is investigated.

Before discussing the distribution of the image gas molecules in the field ion microscope let us refer briefly to the general kinetic theory of gases [10]. Let $f(\boldsymbol{r}, \boldsymbol{p}, t)$ denote the distribution function of the gas molecules, with $\boldsymbol{r}$ representing position, $\boldsymbol{p}$ corresponding to momentum and t to time. The general case, when collisions suffered by the gas molecules are taken into account, corresponds to a transport equation of the form:

$$\mathrm{d}f/\mathrm{d}t = C(f). \tag{1}$$

To characterise the collision process it is necessary to establish the explicit form of the collision integral term, $C(f)$. From the functional dependence of f we have:

$$\partial f/\partial t + \boldsymbol{v} \cdot \operatorname{grad} f - \operatorname{grad} \Phi \cdot \operatorname{grad}_p f = C(f), \tag{2}$$

where $\boldsymbol{v}$ is the velocity, $-\operatorname{grad} \Phi$ is the force exerted on a molecule by an external field related to the potential Φ and grad_p is meant to operate on the $\boldsymbol{p}$ variable.

Some simplification is required in order to apply eq. (2) to our specific problem.

2. Theoretical model

Initially we define the general characteristics of the model intended to represent the imaging gas behaviour in the FIM:

(a) We consider a steady state so that $f(\boldsymbol{r}, \boldsymbol{p}, t)$ will be treated as $f(\boldsymbol{r}, \boldsymbol{p})$.

(b) The gas is under the effect of an electric field resulting from the drop in voltage between tip and screen. The spatial variation of the electric field we will consider is described elsewhere [11]. One model, S, corresponds to a smooth hyperboloidal tip and the other, P, corresponds to a hyperboloidal tip plus a superimposed half sphere protrusion on the top. Model P is meant to simulate the local enhancement of the electric field strength.

The expression to be used for the electric field depends on the model adopted. For a smooth hyperboloidal tip (model S), the electric field strength along the tip symmetry axis is given by:

$$F(z) = F_0 \frac{1}{1 + 2z/R_t}, \tag{3}$$

and for the case of a hyperboloid plus a superimposed half sphere of radius R (model P) it is given by

$$F(z) = F_0\left(\frac{1}{1+2z/R_t} + \frac{2R^3}{z^3}\right). \tag{4}$$

Under the effect of the electric field the gas molecules have a finite probability of being field ionized. Since, under normal operating conditions of the FIM, most of the ionization occurs in a small region (the ionization region) just beyond the critical distance we make an approximation here, restricting the occurrence of ionization to an arbitrarily narrow region as the atom crosses the critical surface.

(c) Our calculations are limited to points along the tip symmetry axis, which corresponds to the z-direction, with $z = 0$ being the top surface and the positive direction taken as from tip to screen.

(d) We do not consider collisions between molecules.

(e) The molecules are considered to originate from one point far away from the tip, z_a, with kinetic energy E_a and with a distribution $W(E_a)$, or $W(p_a)$, as a function of momentum.

(f) As a result of electric polarisation the molecules drift towards the tip, arriving there with a kinetic energy given by the sum of their initial energy, E_a, and the polarisation energy.

(g) When a molecule collides with the surface it tends to accommodate to the tip temperature, T_T. The measure of efficiency in the energy exchange between molecule and metal is characterised by the accommodation coefficient, a_c, as defined by Goodman [12]. On rebounding from the metal surface the molecule is again attracted towards the tip so that several collisions can be expected.

(h) A gas molecule can be ionized when it crosses the ionization zone, either moving towards the tip or moving away from it after rebounding, provided that it rebounds with enough energy to reach the ionization zone. As at each collision the molecule loses energy, at successive crossings of the ionization zone the probability of ionization of one molecule increases. Thus, the molecule's probability of ionization will be considered as a probability that the molecule will be "destroyed", which is proportional to the molecule's "residence time" within the ionization zone. The total number of particles which are ionized at a certain point of the ionization zone is proportional to the local concentration of these particles. We are here assuming a laterally continuous ionization zone. In fact we have disk-like regions [1] disconnected from each other, where the ionization occurs. So, it is possible for the imaging gas molecule to collide with the metal without crossing the ionization region, either when approaching as when going away from the tip. This difficulty appears to us as not significant within the scope of this model and could be

taken into account through an "effective value" for the ionization rate constant.

Now, we put the above considerations into mathematical expressions. The classical accommodation coefficient is expressed [12] as:

$$a_c = (E_i - E_r)/(E_i - E_T), \tag{5}$$

where $E_i \equiv$ incident kinetic energy of the molecule at a certain collision. $E_r \equiv$ scattered, or reflected, kinetic energy corresponding to the same collision as E_i, $E_T \equiv$ average value of E_r for a gas beam scattered at the tip temperature T_T, i.e., E_T would be the average energy of molecules fully accommodated to the tip temperature.

As mentioned before, on average several collisions with the tip are expected for a molecule and since the forces between collisions are conservative the scattered energy of a molecule after the nth collision would correspond to the incident energy for the $(n+1)$th collision. Denoting by E_n the kinetic energy of a gas molecule just after the nth collision (E_0 is the kinetic energy just before the first collision) and using eq. (5) we obtain:

$$E_n = (1 - a_c)E_{n-1} + a_c E_T \tag{6}$$

and

$$E_n = (1 - a_c)^n E_0 + \left[1 - (1 - a_c)^n\right] E_T, \tag{7}$$

If we denote by α_n, the ratio between the gas molecule velocities, after and before the $(n+1)$th collision, we can write:

$$\alpha_0 = (E_1/E_0)^{1/2},$$

$$\alpha_1 = (E_2/E_1)^{1/2},$$

$$\vdots$$

$$\alpha_n = (E_{n+1}/E_n)^{1/2}. \tag{8}$$

According to our previous calculations, the term $C(f)$ is not zero. Its determination must take into account:

(i) the "creation" of particles, away from the tip (at z_a) with momentum $-p_a$, where the minus sign is related with the direction "towards the tip";

(ii) the "destruction" of particles at the ionization zone.

With respect to item (i) we represent the creation of particles at z_a, with momentum -p_a and with distribution $W(p_a)$ as:

$$W(-p_a)\delta(z - z_a)\delta(p + p_a), \tag{9}$$

where δ is the Dirac delta function [13].

Item (ii) refers to the probability of ionization of the gas molecules. Let us

call $\rho(z_c)$ the probability of ionization per unit distance at the critical surface. This can be expressed by

$$\rho(z_c) = P_e(z_c)/v(z_c), \tag{10}$$

where $P_e(z_c) \equiv$ ionization rate constant at z_c, $v(z_c) \equiv$ particle velocity at z_c. The ionization rate constant is field dependent and was calculated using the analytical expression of Haydock and Kingham [14]. For an ionization zone width, w, very small, it is possible to approximate the probability of ionization along w by the product of w times $\rho(z_c)$. Denoting this probability by $P(z_c)$ we write

$$P(z_c) = wP_e(z_c)/v(z_c), \tag{11}$$

or

$$P(z_c) = wP_e(z_c)/[p(z_c)/m]. \tag{12}$$

We will express it simply by

$$P(z_c) = mK/p(z_c), \tag{13}$$

to which corresponds the survival probability

$$S(z_c) = 1 - mK/p(z_c). \tag{14}$$

With these considerations we have to solve eq. (2) expressed with just one spatial coordinate now written as

$$\frac{\partial f}{\partial t} + \frac{p_z}{m}\frac{\partial f}{\partial z} - \frac{\partial \Phi}{\partial z}\frac{\partial f}{\partial p_z} = W(p_a)\delta(z - z_a)\delta(p + p_a) - \frac{mK}{p(z_c)} f\delta(z - z_c). \tag{15}$$

Let us now discuss the collision process between the gas molecules and the metal tip. The collision of one molecule with incident kinetic energy E_n and scattered energy E_{n+1}, can be formally treated as a "destruction" of one particle of energy E_n and a "creation" of another one with energy E_{n+1}. Thus we transform the collision process into a "destruction/creation" one. The relation between E_n and E_{n+1} is as expressed by eq. (6). Thus, the "life" of one molecule lasts, at most, between two successive collisions or, when ionization occurs, between one collision and the ionization time. This is equivalent to separating the distribution function f into an infinite sum of terms f_i, each one corresponding to the fraction of the molecules with energy compatible with the occurrence of i collisions and with initial momentum $-p_a$. Therefore, f_i is not f in eq. (1). Thus:

$$f = \sum_{i=0}^{\infty} f_i, \tag{16}$$

with

$f_0 \equiv$ particles which have not sufferd any collision, and which will disappear at the first collision or before if ionized when crossing the ionization zone;

$f_1 \equiv$ particles originating from the first collision which will last, at most, up to the next collision;

$\vdots$

$f_n \equiv$ particle originating from the nth collision.

We know [7] that the volume element in the phase space, i.e.,

$$d\tau = dz\, dp \tag{17}$$

multiplied by the distribution function $f(z, p)$, is the mean number of molecules in the volume element with values of z and p in the ranges dz and dp, respectively. It is possible then to relate the distribution function for the molecules which had suffered n collisions to the one corresponding to those with $n+1$ collisions, i.e., between f_n and f_{n+1}, respectively. At the metal surface – where the collision occurs – we have:

$$f_n(0, p_n)\, dp_n\, dz = f_{n+1}(0, p_{n+1})\, dp_{n+1}\, dz, \tag{18}$$

where p_n represents the incident momentum corresponding to the kinetic energy E_n. From eq. (8) we have

$$\alpha_n = p_{n+1}/p_n, \tag{19a}$$

and so

$$dp_{n+1} = \alpha_n\, dp_n. \tag{19b}$$

With eq. (19b) into eq. (18) we have

$$f_n(0, p_n) = \alpha_n f_{n+1}(0, p_{n+1}). \tag{20}$$

This relation enables us to construct the distribution f_{n+1} from f_n and successively from f_0.

We assume for now that all particles are "created" at z_a with the same energy E_a. Thus, at a point z, a particle has a definite momentum (in modulus) which is dependent on the position, on the value of E_a and on the number of collisions it had suffered. So,

$$p = p(z, E_a, n), \tag{21}$$

Denoting the *total* energy of a molecule by ϵ, its value after the ith collision, ϵ_i, is dependent on i and E_a, i.e., $\epsilon_i = \epsilon(E_a, i)$ which enables us to write eq. (21) as $p = p'(z, \epsilon_i)$.

Denoting by $\Omega(z, E_a)$ the number of particles at z, with all values of momentum but with the restriction that all particles were "created" with energy E_a, we have:

$$\Omega(z, E_a) = \int_{-\infty}^{\infty} f(z, p, E_a)\, dp. \tag{22}$$

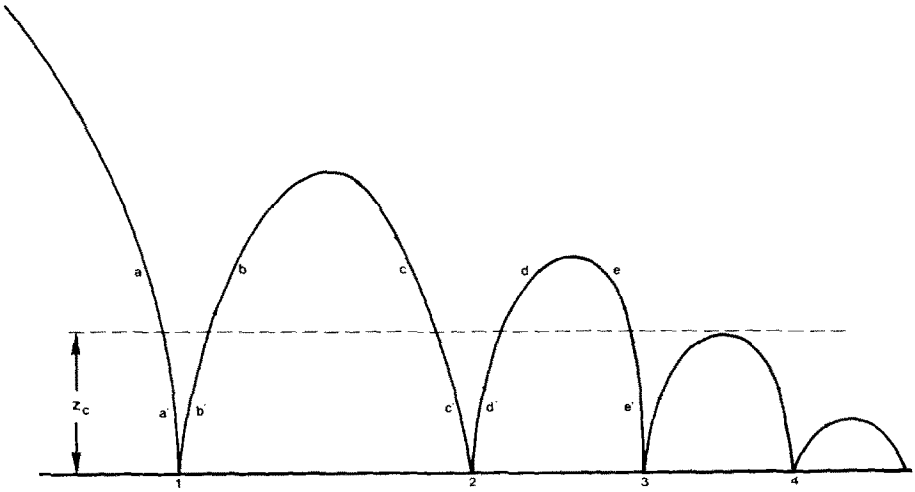

Fig. 1. Schematic view of successive collisions of the imaging gas atom against the tip – here represented by a plane. The dashed line is meant to represent the ionization zone.

Expressing the distribution function as in eq. (16) and the total energy after the ith collision as ϵ_i, we have

$$f(z,\ p,\ E_a) = \sum_{i=0}^{\infty} g_i(z,\ \epsilon_i)\delta\left(p^2/2m + \Phi(z) - \epsilon_i\right), \tag{23}$$

where the delta function ensures the correct relation between momentum, total energy and coordinate z.

In order to obtain an expression for $g_i(z,\ \epsilon_i)$ we must consider the survival probability of a particle, separately for regions $z < z_c$ and $z > z_c$ and for molecules moving towards the tip – momenta denoted by $(-p)$ – and moving away from the tip – momenta denoted by p. The indices 0, 1, 2,... refer to the number of collisions suffered by the molecule and p_c refers to the momentum at the critical distance.

Points $z > z_c$ (see fig. 1)

$i = 0$ (point a – fig. 1)

Survival probability $= 0$, with momentum p,
$= 1$, with momentum $-p$;

i.e., before the first collision the molecule must be approaching the tip.

$i = 1$ (points b and c – fig. 1)

Survival probability $= (1 - Km/p_{c0})(1 - Km/p_{c1})$, with momentum p or $-p$.

$i = 2$ (points d and e – fig. 1)

Survival probability $= (1 - Km/p_{c0})(1 - Km/p_{c1})^2(1 - Km/p_{c2})$, with momentum p or $-p$.

Points $z < z_c$ (see fig. 1)

$i = 0$ (point a′ – (fig. 1)

Survival probability $= 0$, with momentum p,

$= (1 - Km/p_{c0})$, with momentum $-p$.

$i = 1$ (points b′ and c′ – fig. 1)

Survival probability $= (1 - Km/p_{c0})$, with momentum p,

$= (1 - Km/p_{c0})(1 - Km/p_{c1})^2$, with momentum $-p$.

$i = 2$ (points d′ and e′ – fig. 1)

Survival probability $= (1 - Km/p_{c0})(1 - Km/p_{c1})^2$, with momentum p,

$= (1 - Km/p_{c0})(1 - Km/p_{c1})^2(1 - Km/p_{c2})^2$, with momentum $-p$.

Now, from the discussion above and considering the boundary condition which has led to eq. (20) we can write eq. (23), for $z > z_c$, as:

$$
\begin{aligned}
f(z, p, E_a) = {} & H(-p)\delta\left[\frac{p^2}{2m} + \Phi(z) - \epsilon_0\right] \\
& + \frac{1}{\alpha_0}\left(1 - \frac{Km}{p_{c0}}\right)\left(1 - \frac{Km}{p_{c1}}\right)\delta\left[\frac{p^2}{2m} + \Phi(z) - \epsilon_1\right] \\
& + \frac{1}{\alpha_0}\frac{1}{\alpha_1}\left(1 - \frac{Km}{p_{c0}}\right)\left(1 - \frac{Km}{p_{c1}}\right)^2\left(1 - \frac{Km}{p_{c2}}\right) \\
& \times \delta\left[\frac{p^2}{2m} + \Phi(z) - \epsilon_2\right] + \cdots
\end{aligned}
\tag{24}
$$

and for $z < z_c$ as:

$$
\begin{aligned}
& f(z, p, E_a) \\
& = H(-p)\left(1 - \frac{Km}{p_{c0}}\right)\delta\left[\frac{p^2}{2m} + \Phi(z) - \epsilon_0\right] \\
& \quad + \left[H(p) + H(-p)\left(1 - \frac{Km}{p_{c1}}\right)^2\right]\frac{1}{\alpha_0}\left(1 - \frac{Km}{p_{c0}}\right)\delta\left[\frac{p^2}{2m} + \Phi(z) - \epsilon_1\right] \\
& \quad + \left[H(p) + H(-p)\left(1 - \frac{Km}{p_{c2}}\right)^2\right]\frac{1}{\alpha_0}\frac{1}{\alpha_1}\left(1 - \frac{Km}{p_{c0}}\right)\left(1 - \frac{Km}{p_{c1}}\right)^2 \\
& \quad \times \delta\left[\frac{p^2}{2m} + \Phi(z) - \epsilon_2\right] + \cdots,
\end{aligned}
\tag{25}
$$

where $H(x)$ is the Heaviside function and the *total* energies $\epsilon_0, \epsilon_1, \epsilon_2, \cdots$ can

be related to each other by subtracting from each one the potential energy at the metal surface and using eq. (8). Thus,

$$\epsilon_0 = E_a + \Phi(z_a) \tag{26a}$$

and

$$\alpha_n = \left(\frac{\epsilon_{n+1} - \Phi(0)}{\epsilon_n - \Phi(0)} \right)^{1/2}. \tag{26b}$$

The integration of eq. (22), when we substitute into it expression (24) (or (25)), is split into several integrals operating just on the delta function term. As a result of the Heaviside function some integrals are zero in a certain range of p and the result of each integral is multiplied by a coefficient. The integration of the delta function term is done by using the property [13]:

$$\int \delta(g(x))\, \mathrm{d}x = \int \sum_i \frac{1}{|g'(x_i)|} \delta(x - x_i)\, \mathrm{d}x, \tag{27}$$

where x_i is a zero of the function $g(x)$, so that:

$$\int_{-\infty}^{\infty} \delta\left[p^2/2m + \Phi(z) - \epsilon_i \right] \mathrm{d}p = 2m \left\{ 2m \left[\epsilon_i - \Phi(z) \right] \right\}^{-1/2}. \tag{28}$$

We note that some terms of eq. (27) are half of the result above due to a null integrand in the range 0 to $-\infty$ or from $-\infty$ to 0. Substituting eqs. (24) and (25) into eq. (22) and using eq. (26b) we obtain for $z > z_c$:

$$\begin{aligned}
\Omega(z, E_a) = {} & m \left\{ 2m \left[\epsilon_0 - \Phi(z) \right] \right\}^{-1/2} \\
& + \frac{1}{\alpha_0} \left(1 - \frac{Km}{p_{c0}} \right) \left(1 - \frac{Km}{p_{c1}} \right) 2m \left\{ 2m \left[\epsilon_1 - \Phi(z) \right] \right\}^{-1/2} \\
& + \frac{1}{\alpha_0} \frac{1}{\alpha_1} \left(1 - \frac{Km}{p_{c0}} \right) \left(1 - \frac{Km}{p_{c1}} \right)^2 \left(1 - \frac{Km}{p_{c2}} \right) \\
& \times 2m \left\{ 2m \left[\epsilon_2 - \Phi(z) \right] \right\}^{-1/2} + \cdots,
\end{aligned} \tag{29}$$

and for $z < z_c$

$$\begin{aligned}
\Omega(z, E_a) = {} & m \left(1 - \frac{Km}{p_{c0}} \right) \left\{ 2m \left[\epsilon_0 - \Phi(z) \right] \right\}^{-1/2} \\
& + m \left[1 + \left(1 - \frac{Km}{p_{c1}} \right)^2 \right] \frac{1}{\alpha_0} \left(1 - \frac{Km}{p_{c0}} \right) \left\{ 2m \left[\epsilon_1 - \Phi(z) \right] \right\}^{-1/2} \\
& + m \left[1 + \left(1 - \frac{Km}{p_{c2}} \right)^2 \right] \frac{1}{\alpha_0} \frac{1}{\alpha_1} \left(1 - \frac{Km}{p_{c0}} \right) \left(1 - \frac{Km}{p_{c1}} \right)^2 \\
& \times \left\{ 2m \left[\epsilon_2 - \Phi(z) \right] \right\}^{-1/2} + \cdots.
\end{aligned} \tag{30}$$

Up to this point we have considered that all particles were "created" with the same kinetic energy, which is quite unrealistic. In fact, E_a is the kinetic energy of the gas molecule far away from the tip, so it ranges according to a distribution appropriate to the local gas temperature. Hence, the gas density at a point z must take this into account so that the density at a point z, $D(z)$, can be written as

$$D(z) = \int_{E_a} W(E_a)\Omega(z, E_a)\, dE_a, \tag{31}$$

where $W(E_a)$ is a weight function for the number of particles created with kinetic energy E_a at z_a (with momentum $-p_a$). We assume a Boltzmann distribution for the energy of the gas molecules far away from the tip, at a temperature T_G and then:

$$W(E_a) = \frac{2\pi N}{(\pi k_B T_B)^{3/2}} E_a^{1/2} \exp(-E_a/k_B T_G), \tag{32}$$

where k_B is the Boltzmann constant and N is the total number of particles.

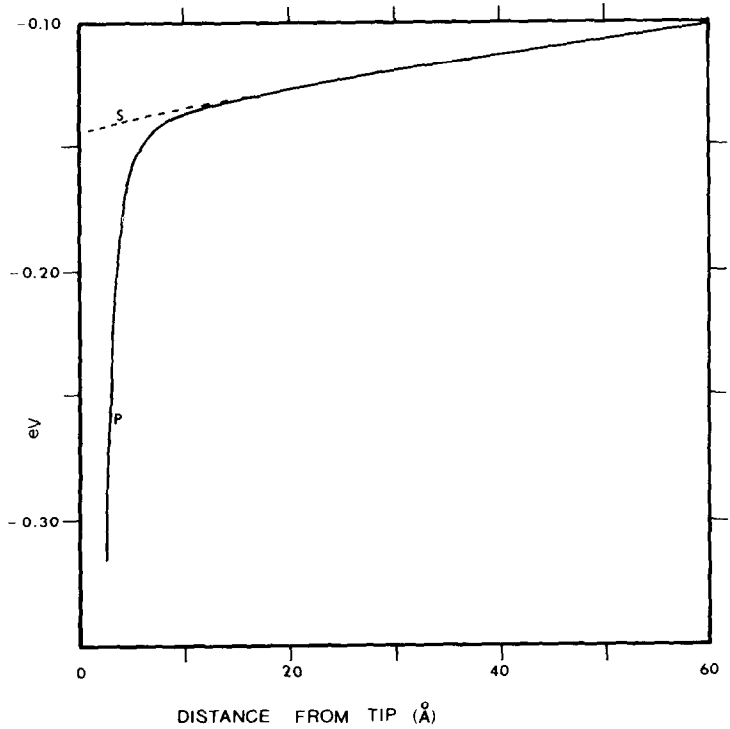

Fig. 2. Potential energy of a polarised gas atom under the influence of the electric field. Model S – dashed line. Model P – full line. $F_0 = 4.5$ V/Å, $T_T = 60$ K and, for model P, $R = 1.58$ Å.

The potential energy, $\Phi(z)$, is calculated considering the effect of the electric field on the molecules. It is known [15] that the amount of work necessary to bring a molecule with permanent dipole moment $\boldsymbol{u}$ and induced dipole moment $\boldsymbol{p}$ into the external field $\boldsymbol{F}$ is given by:

$$W = -(\boldsymbol{u}+\boldsymbol{p})\cdot\boldsymbol{F} + \tfrac{1}{2}\boldsymbol{p}\cdot\boldsymbol{F}, \tag{33a}$$

or

$$W = -\boldsymbol{u}\cdot\boldsymbol{F} - \tfrac{1}{2}\alpha F^2, \tag{33a}$$

where α is the scalar polarisability. We consider the case where $\boldsymbol{u}$ is zero, so just the second term on the right-hand side of the above equation needs to be retained. We choose the position very far away from the tip (infinity) as the reference level for the potential energy, so that

$$\Phi(z) = -\tfrac{1}{2}\alpha[F(z)]^2, \tag{34}$$

where $F(z)$ is the local electric field as discussed in section2.

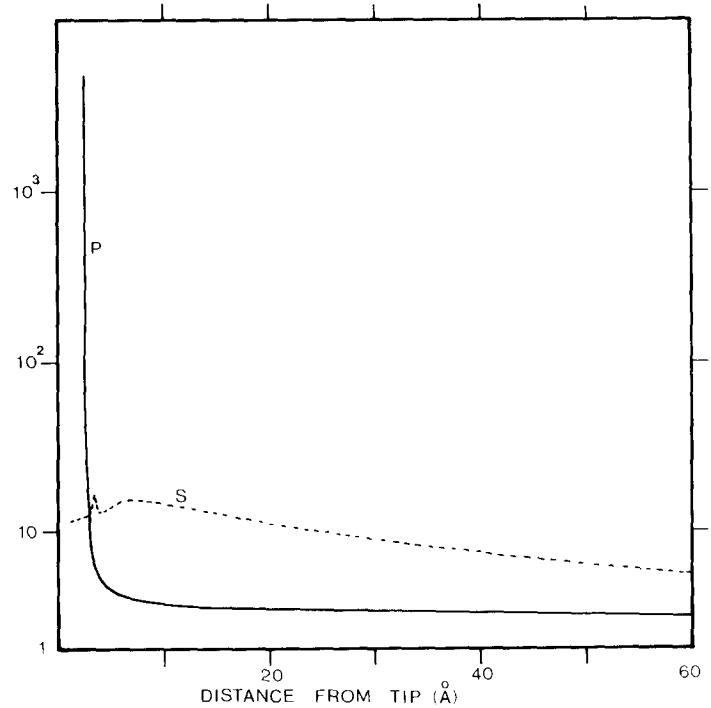

Fig. 3. Concentration enhancement of the gas concentration, relative to a point far away from the tip (z_a), plotted against position. The dashed line corresponds to model S and the full line to model P. $F_0 = 4.5$ V/Å, $T_T = 60$ K and for model P, $R = 1.58$ Å.

3. Numerical results

Our calculations were performed for helium as the imaging gas and a W metal surface. The accommodation coefficient, despite having the possibility of changing with the possible formation of an adsorbed layer, was taken as constant ($a_c = 5 \times 10^{-3}$).

The solution of eq. (31), with $\Omega(z, E_a)$ given by eqs. (29) and (30), must be a numerical one. The integration in the range of energies E_a is made such that

$$\int_0^{\infty} W(E_a)\Omega(z, E_a)\, dE_a \cong \int_0^{E_s} W(E_a)\Omega(z, E_a)\, dE_a, \tag{35}$$

where the upper limit, E_s, was taken as 10 times the average value of E_a, given by:

$$\bar{E}_a = 0.5\, k_B T_G, \tag{36}$$

No significant change was observed if we take E_s as, for example, 20 times the average value of E_a.

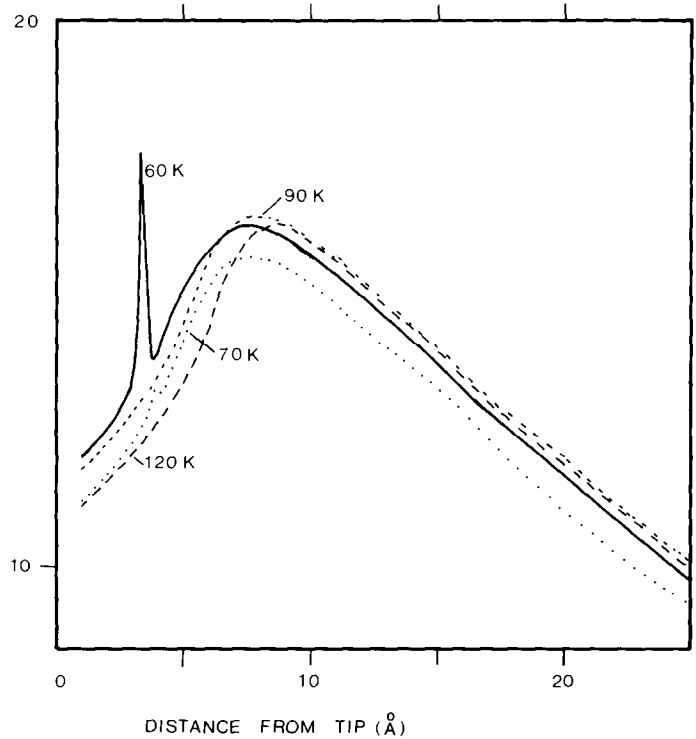

Fig. 4. Concentration enhancement factor versus position in the case of different tip temperatures and $F_0 = 4.5$ V/Å – model S.

As mentioned before, the potential energy was taken as zero at infinity, i.e., far away from the tip surface. In order to determine the kinetic energy at each collision it was necessary to calculate the potential energy at the tip, by use of eq. (34) and the expression for the electric field according to each model (eqs. (3) and (4)). In the case of model P, the very top of the tip corresponds to the coordinate $z = R$ where the field strength is $\cong 3F_0$ due to the rapid increase of $F(z)$ at points very close to the tip in eq. (4). Hence we have calculated the potential energy at the collision as $\Phi(R_G)$, where R_G is a point distant from the tip an amount equal to the radius of the imaging gas. For model S this does not make significant difference because $\Phi(0) \cong \Phi(R_G)$. In model P this procedure avoids unrealistic high (in modulus) values for the potential energy at the tip surface, which would imply too large a kinetic energy. We show in fig. 2 the potential energy for both models, S and P. Fig. 3 represents the enhancement factor of the gas concentration, normalised to the concentration at $z = z_a$, i.e., we represent X, defined as:

$$X(z) = \frac{\text{gas concentration at } z}{\text{gas concentration at } z_a}.$$

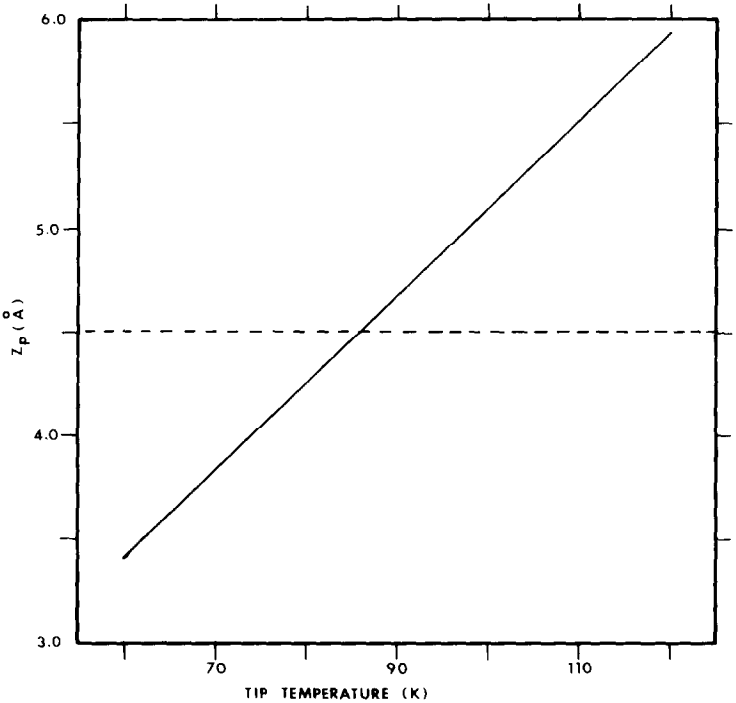

Fig. 5. The values of the maximum height reached by the gas atom after full accommodation, z_p, is plotted against the value of the tip temperature. These calculations for He are for a tip field strength 4.5 V/Å – model S. The dashed line corresponds to the value of the critical distance.

Fig. 3 shows $X(z)$ for both models of the tip shape, S and P. In a certain sense the results for model P are, in this case, unrealistic because this would imply that at all collisions the atom strikes the tip at the very top of a protrusion being strongly accelerated just before the collision and, as a result, having a higher rate of energy lost at each collision. Nevertheless the use of model P is useful to compare the case of collision with a surface with an "average" field F_0, model S, and then to see how the enhancement factor changes between the two cases.

We note that the factor α_n, corresponding to the ratio between the gas atom velocities just after and before a collision (see eq. (8)), tends to 1.0 as n increases. When $\alpha = 1.0$, this corresponds to full accommodation of the gas molecule to the tip temperature. Provided this has occurred, the atom energy does not reduce in further collisions or, in other words, the height reached by the rebounding particle from the metal surface does not decrease. We will denote this height after full accommodation by z_p. If it is less than the critical distance z_c, the particle cannot be "destroyed" any more (by ionization) and we interpret this as the possibility of formation of an "adsorbed layer" over the metal surface. If z_p is greater than z_c, the possibility of ionization –

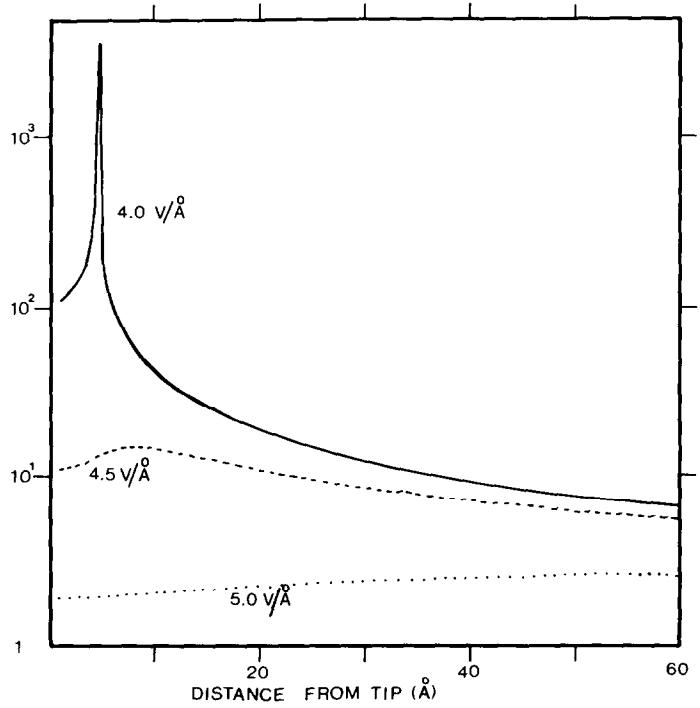

Fig. 6. Concentration enhancement factor versus position for a tip temperature of 70 K and different tip fields – model S.

"destruction" of the particle – still persists and then, as collisions do continue, the survival probability is continuously reduced. In fig. 4 we represent the enhancement factor, X, for model S and different tip temperatures. It is possible to see in fig. 4 that, for a tip temperature equal to 60 K, there is a pronounced peak in the concentration enhancement factor at the point $z = z_p$ which, for this temperature, is less than z_c. What matters here is the occurrence of the peak and not its value which is dependent on an assumed maximum value of bounces. The mentioned peak does not occur when $z_p > z_c$ as, for example in the case of tip temperature equal to 90 or 120 K. In fig. 5 we show, for the same tip field $F_0 = 4.5$ V/Å and model S, the variation of z_p with the tip temperature. The position of the critical distance is also shown. Fig. 6 shows, in the case of model S, the factor X for different values of the tip field strength, F_0. Variation of F_0 causes two opposing effects.

(i) For increasing F_0 the critical distance, z_c, reduces, but the maximum height for a fully accommodated atom, z_p, reduces more rapidly, so that

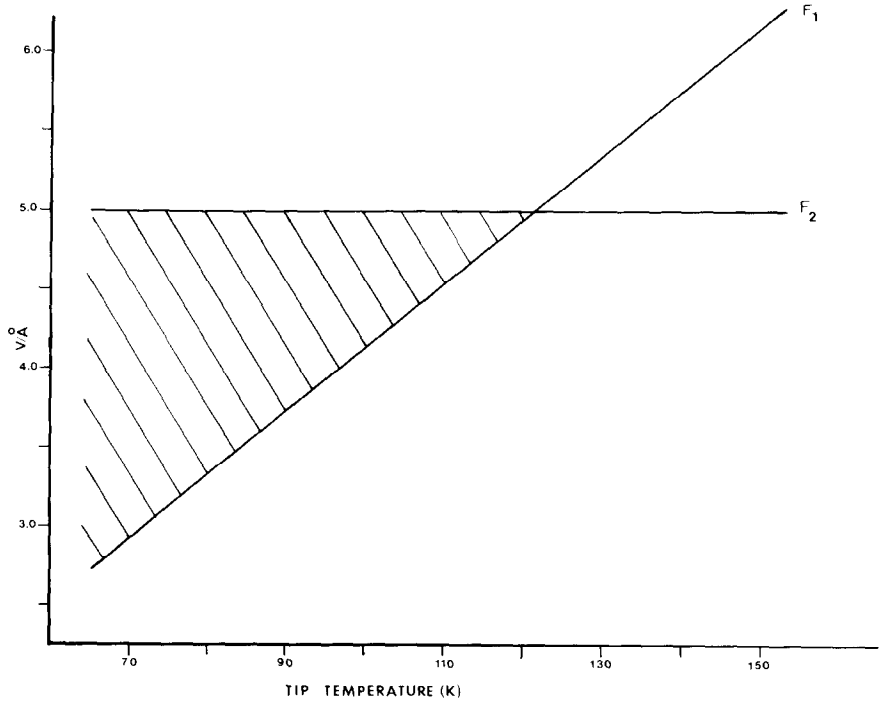

Fig. 7. F_1 is the field at which $z_p = z_c$. Adsorption is restricted to tip fields above this curve. F_2 is the estimated field above which no atoms are fully accommodated to the tip temperature. The dashed region thus corresponds to the range of F_0 for which an adsorbed layer could be formed – model S.

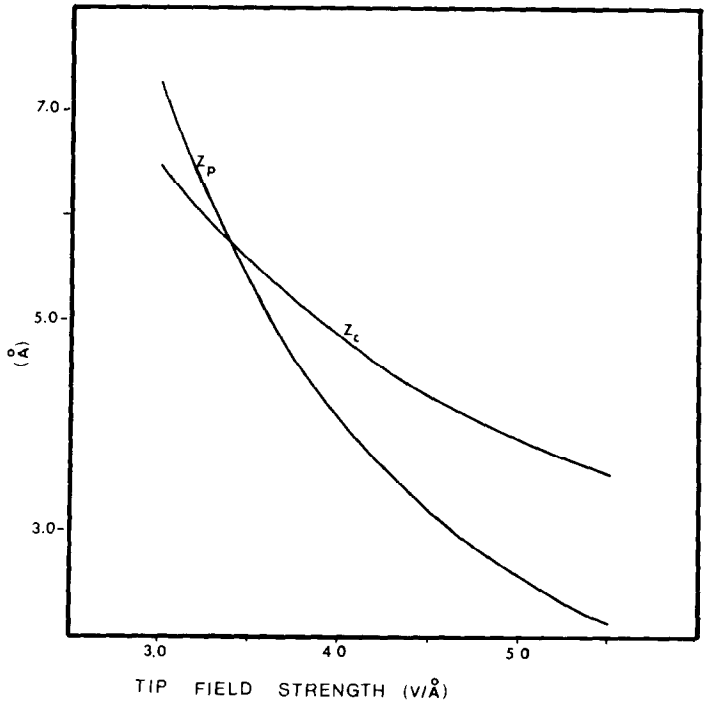

Fig. 8. Variation of the critical distance (z_c) and z_p with the tip field strength. When z_p becomes less than z_c, an imaging gas adsorbed layer could be formed – model S.

adsorption of fully accommodated atoms should occur for F_0 greater than the field at which z_c and z_p are equal.

(ii) For increasing F_0 the ionization rate constant increases, thus increasing the probability of atoms being ionized before they are fully accommodated.

These two effects combine to allow at most only a small range of F_0 in which a field adsorbed layer may occur, as shown in fig. 7, where we have varied the tip temperature and in fig. 8 for different tip fields.

The effect of the tip field strength (or tip voltage) can be analysed by considering the number of collisions the atoms suffer before ionization. Fig. 9 shows, for different values of F_0, the fraction of the total number of ions produced and the number of collisions suffered. In figs. 9a and 9b, the majority of the ions were produced after over 100 collisions. As the tip field is increased the average number of collisions decreases as can be seen in figs. 9c and 9d. The exact values are model dependent and should be considered as an indication of trends rather than in absolute terms.

The amount of ionization occurring on the first few crossings of the ionization zone can be analysed from a different point of view, by considering

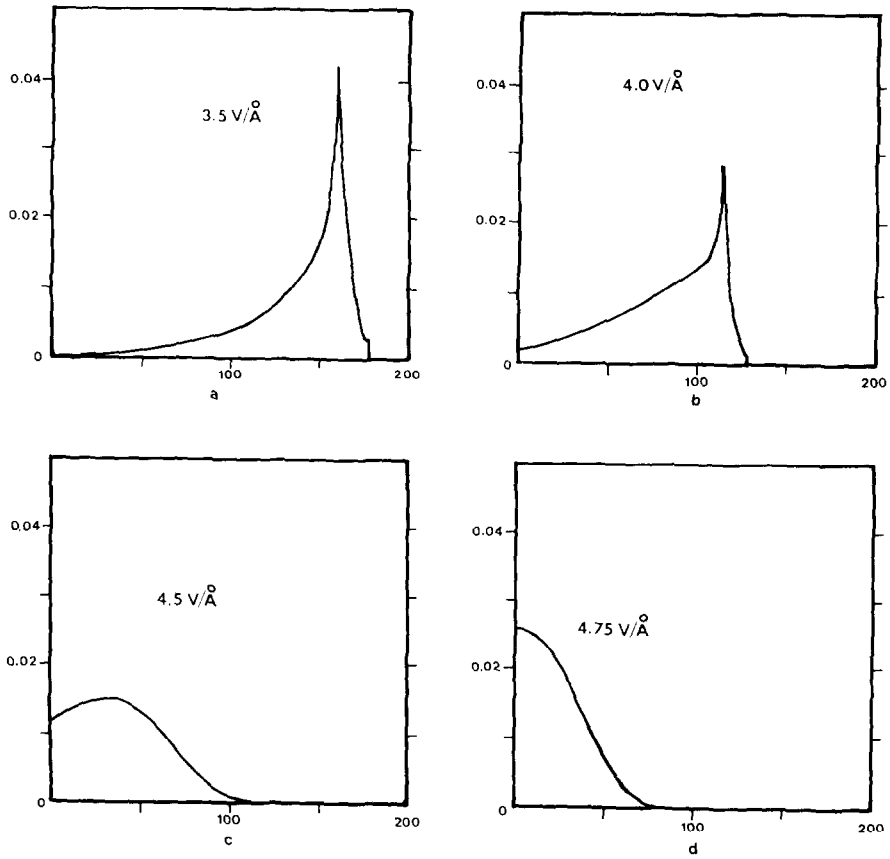

Fig. 9. Fraction of the ions produced after n collisions versus n. Model S, $T_T = 70$ K.

the total energy of the atom when ionization takes place. Considering a population of typical atoms with the average energy $\bar{E}_a$ (eq. (36)) plus the potential energy, we plot in fig. 10 the distribution of the atoms as a function of the total energy they have when ionization occurs. As we increase the tip field (or tip voltage) the distribution broadens significantly.

4. Conclusions

Our calculations show the possibility of formation of an adsorbed layer on the surface, either at low temperature or at low tip field strength. The values of the tip temperature ($\sim$ 70 K) and tip field strength ($\sim$ 4.5 V/Å) at which this occurs are close to the normal operating conditions of the FIM. However, we could not find in the gas concentration any peak which could be associated

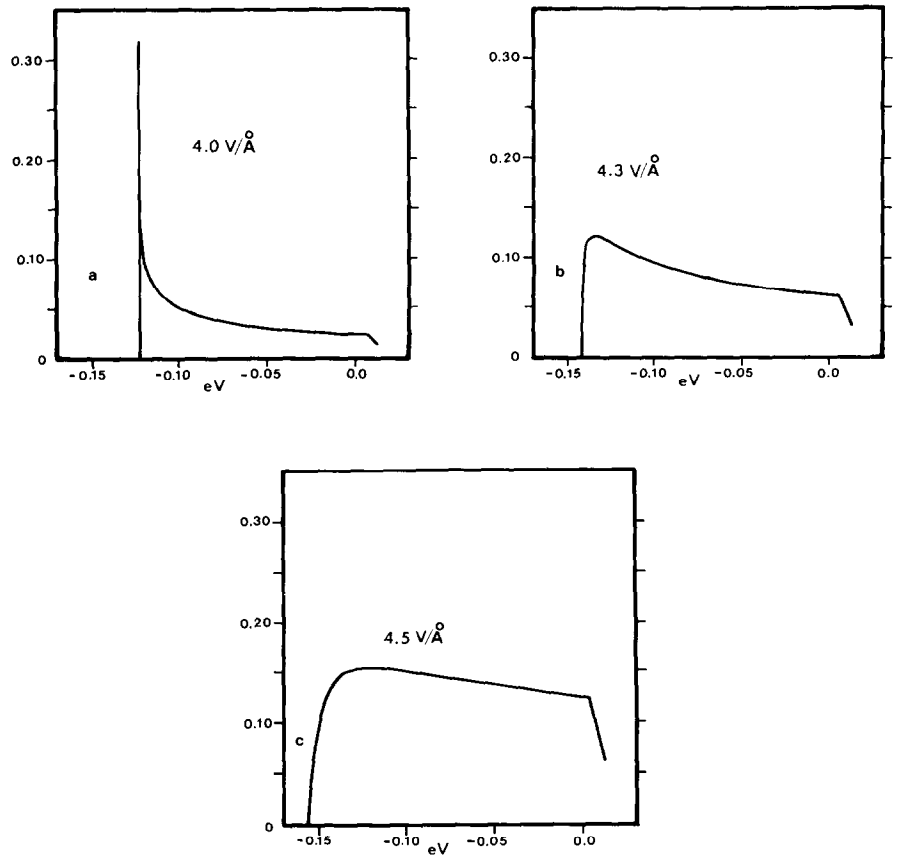

Fig. 10. Fractions of the population of atoms with initial thermal energy E_a plotted against the total energy when ionization occurs – model S.

with the narrow ionization zone width observed in the FIM. A peak in the gas concentration, when it does occur, lies between the tip and ionization zone and, as mentioned, is associated with an "adsorbed layer". For tip temperatures below those corresponding to normal operating conditions of the FIM, $T_T < 70$ K, the peak associated with the "adsorbed layer" formation becomes bigger and closer to the tip as the tip temperature decreases. Our results show the existence of a range of tip field values for which an imaging gas adsorbed layer can be formed. The lower limit, which depends on the tip temperature, is the field for which the ionization zone and the distance z_p (as defined above) are equal. The upper limit is related to the possibility of ionization before accommodation can occur and free space field ionization.

The gas concentration distributions which we have calculated do not have the $\exp(-\frac{1}{2}\alpha F^2)$ Boltzmann factor dependence on local field strength. Indeed

the imaging gas concentration seems to have no clear dependence on local field strength and imaging gas concentration does not necessarily reach a maximum at a point of high local field strength, or at a position corresponding to the ionization zone above a protruding surface atoms. We have thus found, within the limitations of the present method, no evidence which suggests that local variation in imaging gas concentration is the basic mechanism of image formation in the field ion microscope.

References

[1] E.W. Müller and T.T. Tsong, Field Ion Microscopy, Principles and Applications (Elsevier, New York, 1969).
[2] E.W. Müller, CRC Crit. Rev. Solid State Sci. 6 (1976) 85.
[3] R.G. Forbes, J. Microsc. 96 (1972) 57.
[4] R.G. Forbes, J. Microsc. 96 (1972) 63.
[5] J. Duffel and R.G. Forbes, J. Phys. D (Appl. Phys.) 11 (1978) L123.
[6] R.G. Forbes, J. Phys. D (Appl. Phys.) 18 (1985) 973.
[7] H.A.M. van Eekelen, Surface Sci. 21 (1970) 21.
[8] H. Iwasaki and S. Nakamura, Surface Sci. 52 (1975) 588.
[9] H. Iwasaki and S. Nakamura, Surface Sci. 52 (1975) 597.
[10] L.D. Landau and E.M. Lifshitz, Course of Theoretical Physics, Vol. 10, Physical Kinetics (Pergamon, Oxford, 1981).
[11] C.M.C. de Castilho and D.R. Kingham, Surface Sci. 173 (1986) 75.
[12] F.O. Goodman, J. Chem. Phys. 50 (1969) 3855.
[13] E. Merzbacher, Quantum Mechanics (Wiley, New York, 1970).
[14] R. Haydock and D.R. Kingham, Surface Sci. 103 (1981) 239.
[15] J.F. Böttcher, Theory of Electronic Polarisation, Vol. 1 (Elsevier, Amsterdam, 1973).